From X- to O-shaped spatiotemporal spectra of light filaments in water

Miguel A. Porras

Departamento de Física Aplicada, ETSIM, Universidad Politécnica de Madrid, Rios Rosas 21, 28003 Madrid, Spain

Audrius Dubietis and Ernestas Kučinskas

Department of Quantum Electronics, Vilnius University, Saulėtekio Ave. 9, LT-01222, Vilnius, Lithuania

Francesca Bragheri and Vittorio Degiorgio

Department of Electronics, University of Pavia, Via Ferrata 1, 27100 Pavia, Italy

Arnaud Couairon

Centre de Physique Théorique, CNRS UMR 7644, École Polytechnique, F-91128 Palaiseau Cedex, France

Daniele Faccio and Paolo Di Trapani

Istituto Nazionale di Fisica della Materia and Department of Physics and Mathematics, University of Insubria, Via Valleggio 11, IT-22100 Como, Italy

Received July 6, 2005; revised manuscript received August 3, 2005; accepted August 25, 2005

We show that the angle–wavelength spectra of light filaments excited by ultrashort pulses experience a transition from X- to O-like structures when their carrier wavelengths are switched from normal to anomalous dispersion. Calculations confirm that the O-shaped conical emission follows the elliptic geometry of the nonlinear Schrödinger equation with anomalous dispersion. © 2005 Optical Society of America

OCIS codes: 190.5530, 190.7110.

Self-focusing and filamentation of ultrashort pulses in nonlinear media is known to be accompanied by strong conical emission (CE), or angular distribution of wavelengths, observed as colored rings in the far field.[1–3] CE is interpreted as a manifestation of spatiotemporal modulation instability[4] (MI), resulting in a gain profile defined by the dispersive properties of the medium.[4–6] Alternatively, CE has been interpreted as a result of a four-wave mixing (FWM) process underlying the dynamics of the nonlinear Schrödinger equation (NSE), a process that transports energy from pump to idler and signal waves at spatiotemporal frequency bands.[5] With normal dispersion, CE displays rings of increasing radius with increasing detuning from the central wavelength (an X-like structure in an angle–wavelength spectrum). In contrast, the opposite ordering should be displayed with anomalous dispersion[4] (an O-like structure).

In this Letter we report measurements of angle–wavelength (θ–λ) spectra of light filaments in water, demonstrating that CE experiences a transition from X- to O-like structures as the central wavelength is increased from the normal to the anomalous dispersion regime. Though X-like angle–frequency spectra with normal dispersion have been previously measured,[7–10] no observation has been reported in the anomalous regime, and no such kind of elliptical CE has been described to our knowledge. Calculations confirm the development of elliptical CE in a self-focusing wave packet with anomalous dispersion. This CE is found to match the ellipses of maximum gain obtained from MI and FWM analysis, and is consistent with the formation of nonlinear O (NLO) waves,[11] which are conjectured here to play a role similar to that of nonlinear X waves in filamentation with normal dispersion.[12–14]

Figure 1 shows relevant parameters of water. Values of k_0'' were adopted from experimental data, measured by white-light interferometry,[15] yielding zero dispersion at $\lambda \sim 1000$ nm. Our experimental setup allowed measurements in the anomalous region ($\lambda > 1000$ nm) by using a Si-based detector. The absorption curve α was compiled from data for visible[16] and infrared[17] wavelengths.

In the experiment we used a broadly tunable optical parametric generator (TOPAS, Model 4/527, Light Conversion Ltd.) delivering 1 ps pulses in the visible and near infrared. A setup similar to that of Ref. 9 used spatial filtering and focusing by a $f = +500$ mm lens, resulting in a beam waist of 100 μm (slightly wavelength dependent) at the en-

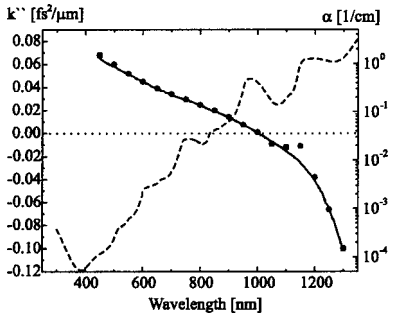

Fig. 1. Group-velocity dispersion k_0'' (dots and solid curve) and absorption coefficient α (dashed curve) of water.

0146-9592/05/243398-3/$15.00

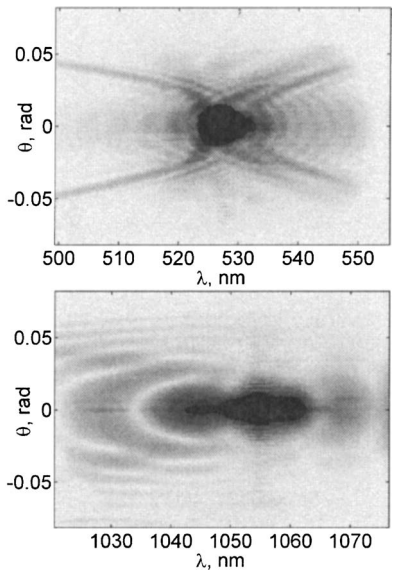

Fig. 2. Angle–wavelength spectra of self-focused 1 ps pulses (top) at 527 nm and 1.6 μJ, (bottom) at 1055 nm and 14.5 μJ carrier wavelength and input energy, respectively.

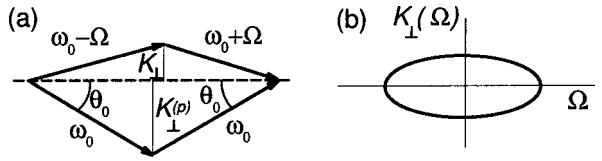

Fig. 3. (a) Vector diagram and (b) values of transverse $K_\perp$ for FWM matching with anomalous dispersion.

trance of a 30 mm long water cell. Within the investigated wavelength range, the incident power was adjusted so as to excite a single filament. Because of enhanced infrared absorption (Fig. 1), the power was significantly higher for the infrared than for the visible.

We characterized the filaments by recording the spectral distribution at the far field with an imaging spectrometer. We focused the output radiation from the exit facet of the cell onto the input plane of the spectrometer (EG&G with 600 lines/mm grating) by means of an achromatic $f=+50$ mm lens. The output plane of the spectrometer was then imaged onto a CCD camera (COHU, 10-bit dynamic range with Spiricon frame grabber) by means of a demagnifying objective ($f=37$ mm). To avoid camera saturation, we blocked the intense peak at the vicinity of the carrier frequencies by placing a small dark screen in the output plane of the spectrometer.

A typical $\theta-\lambda$ spectrum on a logarithmic intensity scale in the normal dispersion region is shown in Fig. 2 (top). At the representative central wavelength of 527 nm, group-velocity dispersion takes the positive value $k_0''=0.056$ fs$^2/\mu$m. Spectra were also recorded at 375, 650, and 900 nm, all within the normal dispersion region and featuring similar X-shaped CE. Further measurements at 527 nm with increasing energies (1.8 and 2.1 μJ) show X patterns that are similar except for an increasing number of X arms. These features are in agreement with recent measurements in the normal dispersion region.[10] At the wavelength of 1055 nm with anomalous dispersion ($k_0''=-0.009$ fs$^2/\mu$m) the $\theta-\lambda$ spectrum apparently develops a multiple annular, or O-like structure (Fig. 2, bottom). This means that the radii of the colored rings at the far field diminish with increasing detuning, thus creating a frequency- and angle-band-limited CE not observed before. This evidences the crucial role played by linear dispersion in the CE of light filaments. At 1090 nm a similar structure is observed, no measurements beyond this limit being possible due to the limit of detection of the Si-based system. We also verified that analogous patterns as in Fig. 2 (bottom) are observed at the slightly smaller and greater input energies of 13.5 and 17 μJ, the O-like spectrum being accompanied by a complex modulation pattern above this energy.

To understand the origin of this CE, we recall its interpretation as a manifestation of a FWM interaction inherent in the NSE dynamics.[5] To extend the analysis in Ref. 5 to the anomalous case, we consider the interaction of two pump waves of frequency and wave number (ω_0, k_0) propagating at small angles $\pm\theta_0=\pm K_\perp^{(p)}/k_0$ from the z direction, with signal and idler waves at $[\omega_0\pm\Omega, k(\omega_0\pm\Omega)]$. Linear phase matching (neglecting nonlinear phase shifts) for maximum FWM efficiency [Fig. 3(a)] leads to

$$K_\perp(\Omega)=\sqrt{2k_0(\delta+k_0''\Omega^2/2)} \tag{1}$$

[Fig. 3(b)] for the transverse part of the idler and signal wave vectors (with $\delta=k_0\theta_0^2/2$). Equation (1), with the changes $\theta\sim K_\perp/k_0$ and $\lambda=2\pi c/(\omega_0+\Omega)$, describes the known X-like (hyperbolic) $\theta-\lambda$ spectrum if $k_0''>0$ and represents an O-like (elliptical) spectrum if $k_0''<0$. Equation (1) is also seen to describe the perturbation modes $(K_\perp,\Omega)$ of maximum gain to the plane-wave solutions of the NSE.[4] We then interpret the observed spectra in anomalous dispersion as a result of a spontaneous spectral reshaping in the self-focusing NSE dynamics toward the elliptical structures specified by Eq. (1).

To support this point and the generality of the process, we performed numerical simulations of the NSE,

$$\partial_z A=\frac{i}{2k_0}\nabla_\perp^2 A-\frac{ik_0''}{2}\partial_\tau^2 A+i\frac{\omega_0 n_2}{c}|A|^2A-\frac{\beta^{(M)}}{2}|A|^{2M-2}A, \tag{2}$$

where $\nabla_\perp^2=\partial_x^2+\partial_y^2$ is the Laplace operator perpendicular to the propagation direction z and n_2 is the nonlinear refractive index. The NSE in Eq. (2) is seen to be the simplest model that captures the features described above and coincides with the model adopted in Ref. 5 except for the multiphoton absorption term ($M=2,3\ldots$ being the order of the process), included here as a mechanism arresting collapse. Higher-order dispersion, plasma effects, Raman scattering, and other effects should be considered for a quantitative description of the process, which is beyond the scope of this Letter. Figure 4 shows $K_\perp-\Omega$ spectra as

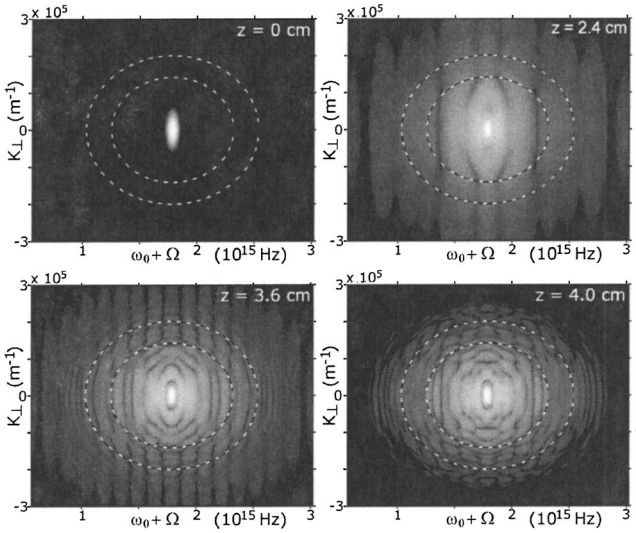

Fig. 4. Calculated $K_\perp - \Omega$ spectra (logarithmic scale, eight decades plotted) of filament in water at 1055 nm at various propagation distances.

the input wave $A=\sqrt{I_0}\exp(-r^2/\Delta w^2-\tau^2/\Delta t^2)$ [$r=\sqrt{x^2+y^2}$, $\Delta w=100$ μm, $\Delta t=85$ fs ($\sim$100 fs FWHM), and $I_0=5.981\times10^{10}$ W/cm^2 (about two critical powers)] at 1055 nm propagates in water ($n=1.32$, $n_2=3.2\times10^{-16}$ cm^2/W, $\beta^{(M)}\simeq2\times10^{-60}$ cm^9/W^5, $M=6$). After the first collapse event ($z\simeq2.4$ cm), the initial Gaussian spectrum gradually develops multiple elliptical rings. The ellipticity $\Delta K_\perp/\Delta\Omega$ of these rings is moreover seen to decrease down to fit, at the latter stages of propagation ($z=3.6, 4.0$ cm), the ellipticity $\sqrt{k_0|k_0''|}=0.267$ fs/μm predicted by Eq. (1) on the basis of the FWM analysis (dashed ellipses in Fig. 4). The superposed, vertical modulations that break and partially mask the rings are clearly due to interference between two temporally split subpulses. Similar behavior is observed with increasing pulse durations ($\Delta t=85, 170, 850$ fs as in the experiment), but owing to the increasingly larger ellipticity imposed by the input Gaussian spectrum ($\Delta t/\Delta r=0.85, 1.7, 8.5$ fs/μm) in comparison with the expected one (0.267 fs/μm), the ellipticity of the formed rings does not reach this lower bound for the longer durations before the breakdown of the filamentary regime.

Note finally that Eq. (1) with $k_0''<0$ also describes the linear asymptotic $K_\perp-\Omega$ spectrum of the NLO waves[11] or conical, stationary solutions of the NSE with $k_0''<0$. A NLO wave is composed of a hot core, where nonlinear effects prevail, surrounded by a weak, linear O wave[18] whose stationarity is sustained by compensation of group-velocity dispersion with cone-angle dispersion $\theta(\Omega)\simeq K_\perp(\Omega)/k_0$. MI then promotes the amplification of the $(K_\perp,\Omega)$ pairs necessary for NLO wave generation, if coherence among the spectral components is preserved. A similar mechanism was shown to be responsible for the formation of nonlinear X waves with normal dispersion, which have been indeed observed in far- and near-field measurements.[13,14]

In short, we demonstrated experimentally a transition of the spatiotemporal spectra of light filaments from X- to O-shaped structures as material dispersion changes its sign. Numerical simulations of the NSE showed that the spectrum of the self-focusing pulse is driven by the FWM or MI mechanisms toward the ellipses of highest gain imposed by anomalous material dispersion.

Authors acknowledge support from Sixth EU Framework Programme contract RII3-CT-2003-506350 (Laser-lab Europe), the Acción Integrada Hispano-Italiana HI2004-0078, and Ministero dell'Istruzione, dell'Università e della Ricerca COFIN-04 FIRB-01 projects. M. A. Porras's e-mail address is miguelangel.porras@upm.es.

References

1. E. T. J. Nibbering, P. F. Curley, G. Grillon, B. Prade, M. Franco, F. Salin, and A. Mysyrowicz, Opt. Lett. **21**, 62 (1996).
2. A. Brodeur, F. A. Ilkov, and S. L. Chin, Opt. Commun. **129**, 193 (1996).
3. B. D. Paul, M. L. Dowell, A. Gallagher, and J. Cooper, Phys. Rev. A **59**, 4784 (1999).
4. L. W. Liou, X. D. Cao, C. J. McKinstrie, and G. P. Agrawal, Phys. Rev. A **46**, 4202 (1992).
5. G. G. Luther, A. C. Newell, J. V. Moloney, and E. M. Wright, Opt. Lett. **19**, 789 (1994).
6. E. J. Fonseca, S. B. Cavalcanti, and J. M. Hickmann, Opt. Commun. **169**, 199 (1999).
7. D. Strickland and P. Corkum, J. Opt. Soc. Am. B **11**, 492 (1994).
8. D. Mikalauskas, A. Dubietis, and R. Danielius, Appl. Phys. B: Lasers Opt. **75**, 899 (2002).
9. A. Dubietis, G. Tamošauskas, I. Diomin, and A. Varanavičius, Opt. Lett. **28**, 1269 (2003).
10. D. Faccio, P. Di Trapani, S. Minardi, A. Bramati, F. Bragheri, C. Liberale, V. Degiorgio, A. Dubietis, and A. Matijosius, J. Opt. Soc. Am. B **22**, 862 (2005).
11. M. A. Porras, A. Parola, and P. Di Trapani, J. Opt. Soc. Am. B **22**, 1406 (2005).
12. P. Di Trapani, G. Valiulis, A. Piskarskas, O. Jedrkiewicz, J. Trull, C. Conti, and S. Trillo, Phys. Rev. Lett. **91**, 093905 (2003).
13. D. Faccio, A. Matijosius, A. Dubietis, R. Piskarskas, A. Varanavičius, E. Gaizauskas, A. Piskarskas, A. Couairon, and P. Di Trapani, Phys. Rev. E **72**, 037601 (2005).
14. D. Faccio, M. A. Porras, A. Dubietis, F. Bragheri, A. Couairon, and P. Di Trapani, "Conical emission, pulse splitting and X-wave parametric amplification in Kerr media," submitted to Phys. Rev. Lett.
15. A. G. Van Engen, S. A. Diddams, and T. S. Clement, Appl. Opt. **37**, 5679 (1998).
16. L. Kou, D. Labrie, and P. Chylek, Appl. Opt. **32**, 3531 (1993).
17. H. Buiteveld, J. M. H. Hakvoort, and M. Donze, in Proc. SPIE **2258**, 174 (1994).
18. M. A. Porras and P. Di Trapani, Phys. Rev. E **69**, 066606 (2004).